Korean J. Chem. Eng., 36(6), 954-964 (2019)
DOI: 10.1007/s11814-019-0271-5

pISSN: 0256-1115
eISSN: 1975-7220

Multiple transesterifications in a reactive dividing wall column integrated with a heat pump

Heecheon Lee, Wonjoon Jang, and Jae W. Lee†

Department of Chemical and Biomolecular Engineering, Korea Advanced Institute of Science and Technology (KAIST), 291 Daehak-ro, Yuseong-gu, Daejeon 34141, Korea
(*Received 12 February 2019 • accepted 8 April 2019*)

Abstract−This study addresses a reactive dividing wall column (RDWC) integrated with a vapor recompression heat pump (VRHP). The reaction applied to the system contains two consecutive transesterifications of dimethyl carbonate (DMC) and ethanol, which yields methanol (MeOH) as a by-product, ethyl methyl carbonate as an intermediate product and diethyl carbonate (DEC) as the final desired product. DEC is the only stable node of the five component reacting mixture. The location of the reaction region and feed stages affects the purity of the top product because the unstable node product is not pure MeOH but DMC-MeOH azeotrope. The VRHP pressurizes the top gas product stream and the compressed gas provides heat to the bottom stream of the ethanol recovery section. The optimization procedure minimizes the power consumption of the compressor with respect to the gas flow rate. The energy consumption in the RDWC integrated with a VRHP is reduced by 32.1% and the total utility cost is also cut by 21.6% compared with the conventional RDWC.

Keywords: Reactive Dividing Wall Column, Vapor Recompression Heat Pump, Diethyl Carbonate, Multiple Reactions, Energy Savings

INTRODUCTION

Distillation, a major process for separating pure components from a liquid mixture, is the significant part of the chemical industry. Considerable combustion of fossil fuels is required for energy intensive distillation which accounts for more than 10% of global energy consumption [1]. Consequently, in addition to the development of techniques of CO_2 capture and utilization [2-6], the reduction of energy consumption in distillation is an essential issue for mitigating carbon dioxide greenhouse emissions.

Various energy-efficient techniques exist for distillation to produce high quality products [7-9]. Reactive distillation (RD) can reduce energy consumption and yield a product of high purity by integrating distillation and reaction into one physical shell [10,11]. Because of this distinctive strength of RD, studies have focused on the design and feasibility evaluation of RD for binary or multi-component reactive systems using phase and reaction equilibrium information [12-16]. In particular, RD systems with multi-components and multi-reactions necessarily involve more recovery distillation columns [17], which increases energy consumption. Hence, a reactive dividing wall column (RDWC) was designed by integrating the conventional RD column and additional non-reactive purification columns into a single shell column to further reduce energy consumption [18,19].

Recently, a reactive dividing wall column (RDWC) has been studied for its high thermodynamic efficiency and low cost [18-20]. However, the reduction in energy consumption may not be significant in the RDWC because its energy consumption is influenced by the position of the reaction region and dividing wall. The reaction region is located differently according to the dynamic properties of the reaction products in the phase diagram [12,14]. For example, the diethyl carbonate (DEC) production system by two consecutive transesterifications in the RDWC is available because the desired product is the stable node that has the highest boiling point [21]. The reaction region is preferably located at the bottom of the RDWC to separate pure methanol (MeOH) as a by-product if the reaction between ethanol (EtOH) and dimethyl carbonate (DMC) completely consumes DMC by using excess EtOH. Then the unstable node of a minimum azeotrope between DMC and MeOH is eliminated [22]. Moreover, the bottom of the RDWC is completely partitioned for recovery of excess EtOH in the non-reactive section. Thus, the RDWC requires two reboilers and one condenser and still consumes a large amount of energy.

There has also been an attempt to further diminish energy consumption using a vapor recompression heat pump (VRHP) [23-26]. The VRHP consists of two steps [27]. The first step elevates the temperature of the overhead vapor using a compressor. The second step utilizes the latent heat for reboiling the bottom stream of the column. However, the VRHP integrated system is primarily employed in non-reactive systems [23,24] or simple RD systems with a single reaction [25,26] because the design of the VRHP integrated RD, which includes multiple reactions, is challenging due to its complexity and a large number of optimization variables.

This study demonstrates the integration of the VRHP with an RDWC for consecutive multi-component reactions to explore whether this integration leads to achieving the reduction of energy

†To whom correspondence should be addressed.
E-mail: jaewlee@kaist.ac.kr

consumption and utility cost. Two consecutive transesterifications of DMC and EtOH were selected for this study with ethyl methyl carbonate (EMC) as an intermediate and DEC as the final desired product. Since DEC is the only stable node with the highest boiling point, it is feasible to remove pure DEC at the bottom of the reactive section in the RDWC. We demonstrate that the VRHP integrated RDWC utilizes the compression of the upper MeOH stream, and it provides heat for the bottom stream of the EtOH recovery column. The optimization of energy consumption in the integrated system is carried out by manipulating the gas influx into the compressor for the minimization of the power consumption of the compressor. Finally we show how the VRHP integrated RDWC reduces energy consumption and operating costs over the conventional RDWC with the production of high purity products despite the presence of multiple reactions.

THERMODYNAMIC AND KINETIC MODEL

1. Thermodynamic Model for the DEC Reacting Mixture

The UNIQUAC activity coefficient model was adopted to simulate the equilibrium behavior of the liquid and gaseous components. The thermodynamic parameters in this study were newly regressed to make the equilibrium behavior of the components similar to the actual data in the literature [28-31]. The properties of DMC, DEC, EtOH, and MeOH were extracted from Aspen Plus™. EMC, which is not in the data bank of Aspen Plus™, was directly added to the Aspen Plus™ component data with the molecular structure in the NIST Chemistry WebBook [32]. Experimental data in the previous studies were collected and the regression was performed for each binary pair using Aspen Plus™. Experimental data used in the regression include (i) DMC+EtOH and DMC+MeOH by Rodriguez et al. [28], (ii) DEC+EtOH and DEC+MeOH by Rodriguez et al. [29], and (iii) EtOH+EMC, EMC+MeOH, EMC+DEC, and EMC+DMC obtained by Zhang et al. [30]. In addition, binary experimental data for (iv) MeOH+DMC, EtOH+DMC, EtOH+DEC, DMC+DEC and EtOH+EMC by Luo et al. [31] were added to vapor-liquid equilibrium data for all binary pairs. Table 1 shows the parameters calculated through the regression and the graphs of assembled vapor-liquid equilibrium data are included in the Supporting Information (Fig. S1).

2. Kinetic Model for the DEC Production

DEC was synthesized via two sequential transesterification reactions started from DMC and EtOH [33]. In the first transesterification, DMC and EtOH reacted to form MeOH and an intermediate product of EMC. Subsequently, EMC reacted with EtOH to produce MeOH and DEC. The disproportionation reaction of two EMC molecules to form DEC and DMC was ignored because it did not significantly occur as reported by Keller et al. [34]. Accordingly, the production process of DEC is represented by the following two-step reactions:

$$\mathrm{DMC+EtOH \leftrightarrow EMC+MeOH} \quad (1)$$

$$\mathrm{EMC+EtOH \leftrightarrow DEC+MeOH} \quad (2)$$

The rate equation for the first and second transesterification reactions under a homogeneous catalyst of sodium ethoxide is expressed as [34]:

$$r_{R1}=x_{cat}\left[1.34\times10^{11}e^{\frac{-36530}{RT}}a_{DMC}a_{EtOH} - 1.338\times10^{11}e^{\frac{-38480}{RT}}a_{EMC}a_{MeOH}\right] \quad (3)$$

$$r_{R2}=x_{cat}\left[1.8\times10^{13}e^{\frac{-54620}{RT}}a_{EMC}a_{EtOH} - 3.08\times10^{13}e^{\frac{-53680}{RT}}a_{DEC}a_{MeOH}\right] \quad (4)$$

r_{R1} and r_{R2} are the rate of the first and second transesterifications started from DMC with EtOH, respectively, and x_{cat} is the mole fraction of the homogeneous catalyst (x_{cat}=0.005). Pre-exponential factors (unit: mol m^{-3} s^{-1}) and activation energies (unit: kJ mol^{-1}) are described in the above equations. a_i is the activity for component i, denoted as the product of the activity coefficient and mole fraction, $a_i=\gamma_i x_i$.

PROCESS DESIGN OF ENERGY SAVING IN MULTIPLE REACTIONS

1. Feasibility of the DEC Production Reaction as Multiple Reactions in RD

The reactions of DEC formation occur in the reactive trays instead of packed beds [35] and the reaction system includes five components and three azeotropes. The boiling points and stabilities of the components and the azeotropes are given in Table 2. DEC is the sole stable node, while the unstable nodes are the DMC-MeOH and EMC-EtOH binary azeotropes [22]. Therefore, this quinary system has two distillation regions with a common stable node because one distillation region should contain a pair of a stable node and an unstable node [36]. DEC is reachable from the two distillation regions and can be removed as a bottom product of the RD column according to the feasibility criteria of RD [12,15,16]. How-

Table 1. UNIQUAC parameters for the DEC production system

Component i	EtOH	EtOH	EtOH	EtOH	MeOH	MeOH	MeOH	DMC	DMC	DEC
Component j	MeOH	DMC	DEC	EMC	DMC	DEC	EMC	DEC	EMC	EMC
Temperature units	°C	°C	°C	°C	°C	°C	°C	°C	°C	°C
A_{ij}	−2.27942	3.985909	−1.38135	1.185983	1.887619	0.766061	0.049784	−2.39287	0.823543	3.971585
A_{ji}	1.778826	−2.65204	1.590663	−5.18203	0.1849	0.666349	1.693394	0.292677	−0.28749	−1.93703
B_{ij}	725.7728	−1442.62	497.9691	−454.899	−626.115	−158.329	22.35887	459.2484	−201.006	−1842.6
B_{ji}	−573.891	795.333	−743.423	1680.466	−390.549	−737.757	−942.568	147.6238	−23.4868	971.9152

Table 2. Boiling points and stabilities of the components and azeotropes in the quinary system for the DEC production at 1 atm

Component (or Azeotrope)	Temperature (°C)	Stability
DMC (14.45%)+MeOH (85.55%)	63.70	Unstable node
MeOH	64.53	Saddle
DMC (30.22%)+EtOH (69.78%)	75.39	Saddle
EMC (7.93%)+EtOH (92.07%)	77.90	Unstable node
EtOH	78.31	Saddle
DMC	90.22	Saddle
EMC	107.70	Saddle
DEC	126.82	Stable node

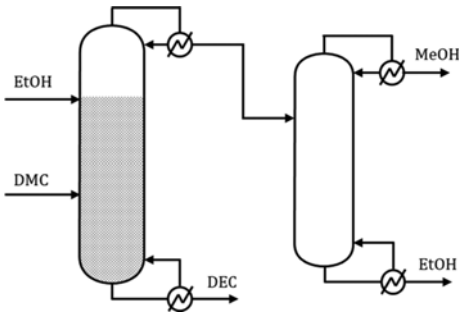

Fig. 1. The conventional RD system for DEC production [37]. The marked area represents a reaction region.

ever, all other components form minimum azeotropes, and two of these azeotropes are unstable nodes in each distillation region. Therefore, withdrawing a light product with a high purity is limited in each distillation region.

In the DEC production system, when an excess reactant of EtOH is fed into the reaction section, DMC is a limiting reactant and totally consumed by the reaction because the removal of DEC at the bottom drives the two consecutive reactions to the forward direction. Then, the phase equilibrium behavior dominates EtOH, MeOH, EMC, and DEC without DMC. In this quaternary system, MeOH is the only unstable node and DEC is the sole stable node. Therefore, the integration of these two reactions and V-L phase equilibrium can produce pure products.

2. Upper and Lower RDWC Systems for the DEC Production

In a distillation system, all product streams need to be separated into pure components. However, in the DEC production system,

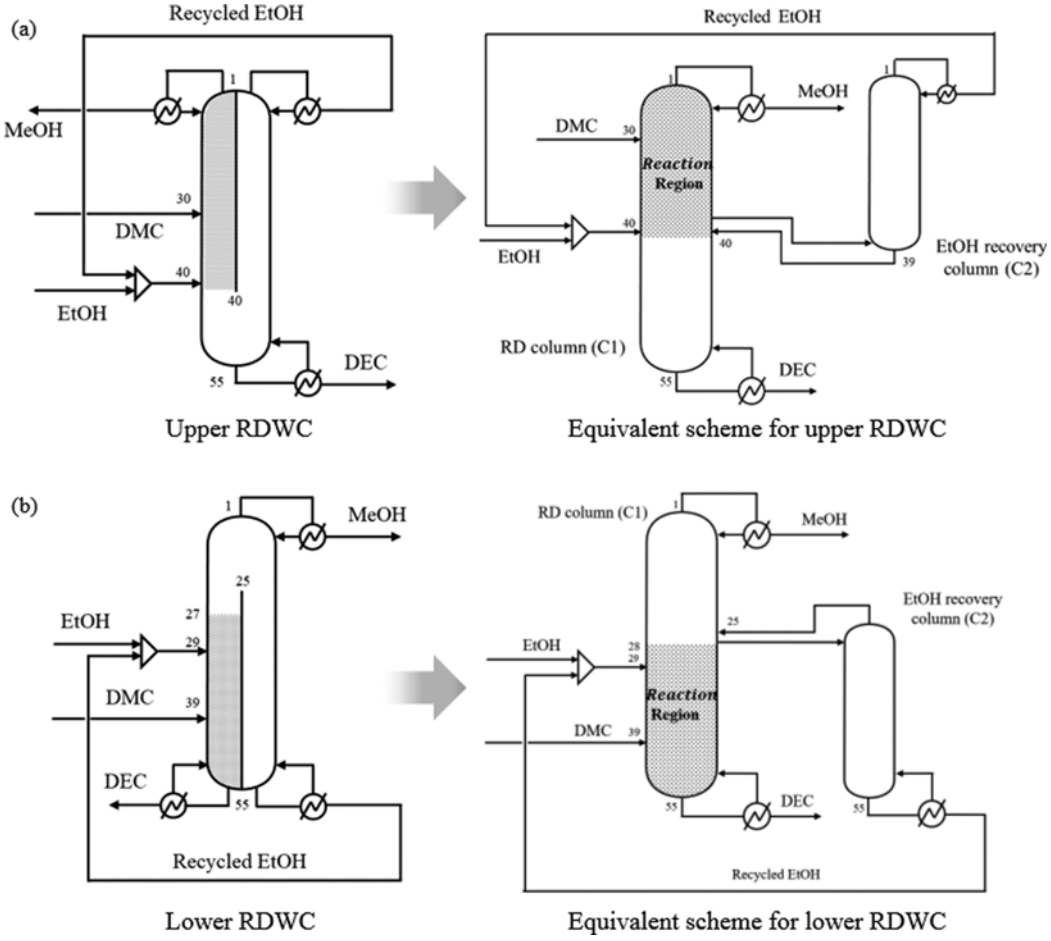

Fig. 2. (a) The upper RDWC and the equivalent scheme consisting of an RD column (C1) and an EtOH recovery column (C2) for the upper RDWC. (b) The lower RDWC and the equivalent scheme for the lower RDWC. The marked areas represent reaction regions in each system.

the azeotropic mixture tends to form in the top product because the azeotrope between DMC and MeOH is an unstable node with the lowest boiling point. In order to separate only MeOH as a top product, DMC should be consumed by the reaction and not be present in the rectifying section. Hence, excess EtOH reacts with DMC and is recycled into the reaction region for the high conversion of DMC. In the conventional RD system, the DMC feed stage is located in the bottom of the reaction region [37] as shown in Fig. 1. However, since the coexistence of the two reactants in the reactive section can generally yield a high conversion, the DMC feed stage needs to be properly positioned [21] with respect to the location of the reaction region and the dividing wall in the RDWC (Figs. 2(a) and (b)).

2-1. Comparison of the Upper and Lower RDWCs for the DEC Production System

We investigated both the upper and lower RDWCs to determine the energy-efficient configuration and the effect of the DMC feed location on the composition profile behavior. The RDWCs were simulated using Aspen Plus^{TM} with the kinetic model [34] and the newly regressed thermodynamic parameters. The simulated equivalent schemes divided into an RD column and an EtOH recovery column are shown in Fig. 2. The differences between the upper and the lower RDWCs for the DEC production are the positions of the reaction region, the dividing wall, and the feed stages of the reactants. Most of DMC is consumed in the reaction region, but the traces of DMC are included in the product stream depending on the DMC feed stage. Therefore, the DMC composition profile according to the location of the feed stage needs to be considered when the upper and the lower RDWCs are designed.

The upper RDWC in Fig. 3(a) has a reaction region at the top and MeOH is recovered at the top of the reactive section while DEC is produced at the bottom. Excess EtOH is recovered from the top non-reactive section and is recycled to the reactive section. Thus, EtOH dominates the reaction region and the temperature of the reaction region is near or below the boiling point of EtOH in Fig. 4(a). Therefore, the purity of MeOH at the top reactive section depends on the distribution of DMC in the reaction region according to the DMC feed stage location. The feed stages of EtOH and DMC were determined by the sensitivity analysis to minimize the DMC mole fraction of the MeOH stream because pure MeOH instead of MeOH-DMC azeotrope should be produced at the top of the reactive section in Fig. 4(c). The purity of MeOH increases as the DMC feed position is lowered. However, if DMC is injected into the bottom of the reactive section, the conversion decreases. In order to prevent the low conversion, DMC was fed upward into the middle of the reactive section in a way that did not affect the MeOH stream purity, while EtOH was provided to the bottom reactive section. As shown in the composition profile (Fig. 4(b)), there was no DMC in the top reactive section and MeOH was produced with a purity of 99.5%. However, a high reflux ratio and energy consumption are necessary to produce high purity MeOH in the upper RDWC because the separation of MeOH and the reaction of DMC need to simultaneously occur in the reaction region.

For the lower RDWC in Fig. 3(b), the reaction region is located at the bottom of the RDWC and the recovery of MeOH and EtOH occurs in the non-reactive section. Excess EtOH dominantly exists

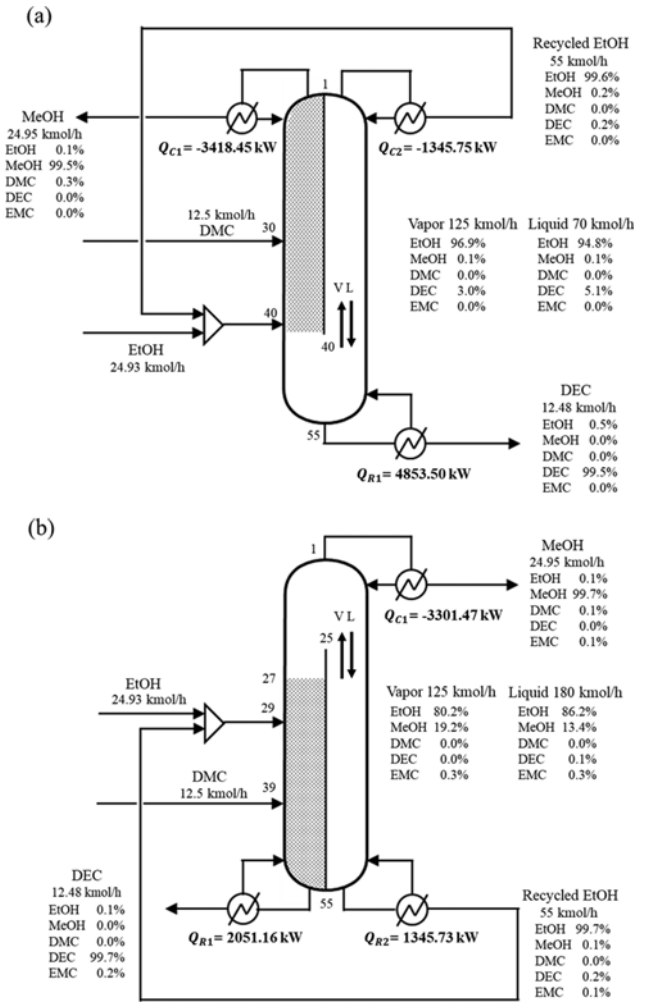

Fig. 3. (a) The upper RDWC consisting of the top reactive section and non-reactive section for an EtOH recovery and a DEC separation, and (b) the lower RDWC consisting of the bottom reactive section and non-reactive section for a MeOH and EtOH recovery. The marked areas represent reaction regions.

in the reaction region except for the lower part of the reaction region where DEC with the highest boiling point is produced as a desired product. In order to recover MeOH and EtOH in the non-reactive section, there should be no DMC in the upper reaction region because the lower boiler of the DMC-MeOH azeotrope will be produced at the top of the non-reactive section. Therefore, we performed a sensitivity analysis to minimize the DMC mole fraction in the side liquid stream flowing to the non-reactive section. Fig. 5(c) shows the result in which the DMC mole fraction in the side liquid stream tended to decrease at a lower DMC feed stage and an upper EtOH feed stage. In a way similar to that of the upper RDWC, DMC was fed into the middle of the reactive section in a way that did not affect the purity of the side-liquid stream, while the EtOH feed stage was placed at the top reactive section. The composition profiles in Fig. 5(b) confirmed that there was no DMC in the non-reactive section. In other words, the reaction region for the consecutive transesterifications and the recovery region of MeOH and EtOH can successfully be separated. This separation

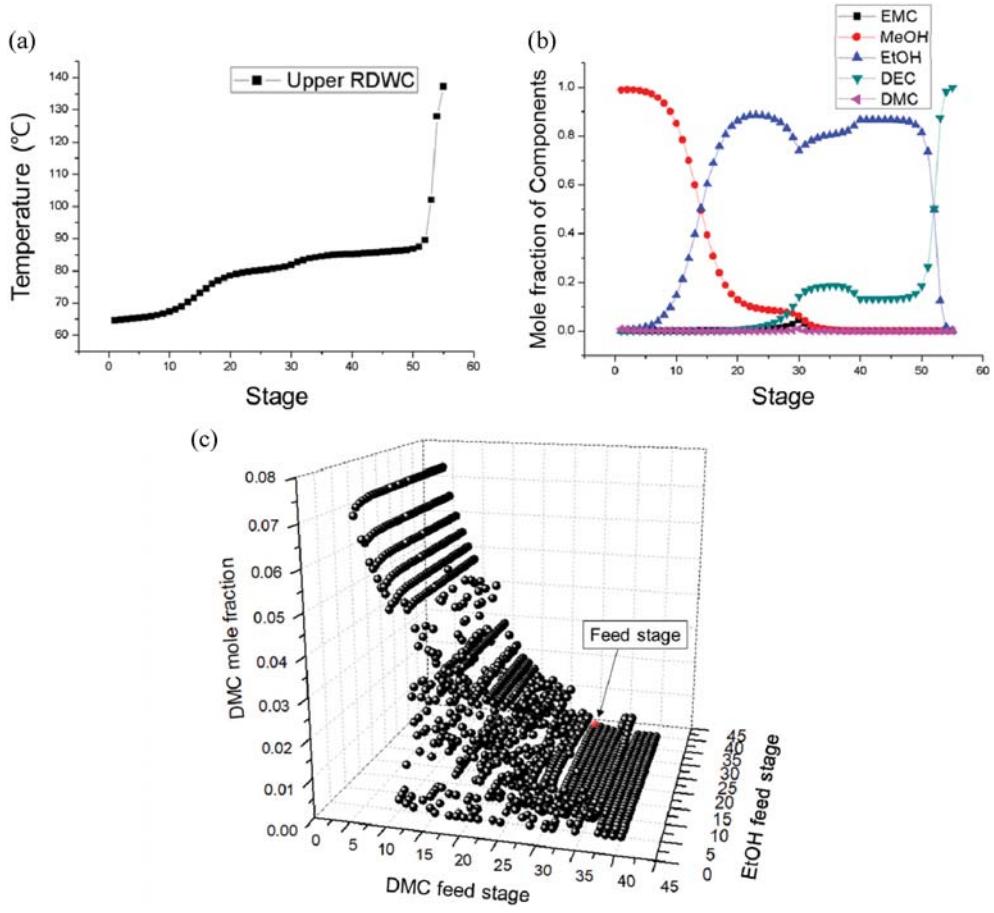

Fig. 4. (a) The temperature profile and (b) the composition profile in the RD column of the upper RDWC, and (c) sensitivity results of the DMC mole fraction in the MeOH stream according to the change of the DMC and the EtOH feed stages.

Table 3. Operating conditions, product purities, energy consumptions and cost evaluations of the upper and the lower RDWCs

Parameter	Upper RDWC	Lower RDWC
Condenser pressure [atm]	1	1
Pressure drop [kPa]	0.7	0.7
Bottoms rate of C1 [kmol/h]	12.48	12.46
Distillate rate of C1 [kmol/h]	24.95	24.97
Reflux ratio of C1	13	12.5
Distillate rate of C2 [kmol/h]	55	125
Bottoms rate of C2 [kmol/h]	70	55
DEC purity [mol%]	99.5	99.7
MeOH purity [mol%]	99.5	99.7
EtOH purity [mol%]	99.7	99.7
Q_{C1} [kW]	−3418.45	−3301.47
Q_{R1} [kW]	4853.50	2051.16
Q_{C2} [kW]	1345.75	-
Q_{R2} [kW]	-	1345.73
Q_{Total} [kW]	9617.70	6698.36
Total capital cost ($10^3$$)	2865.90	2371.2
Total utility cost ($10^3$$/yr)	1469.00	1039.67
TAC ($10^3$$/yr)	2424.30	1830.07

of the two regions allows EtOH and MeOH to be recovered with a relatively low reflux ratio and energy consumption compared to the upper RDWC case.

The operating conditions and simulation results of the upper and the lower RDWC are presented in Table 3. The simulation results contain the mole purity of the products, the energy consumption in the reboilers and condensers of the RDWCs, and the cost evaluations. Both of the RDWC configurations can produce DEC and MeOH with a purity higher than 99.5 mol%. However, the upper RDWC requires a high reflux ratio compared to the lower RDWC because both MeOH recovery and consumption of DMC by reaction should be done in the upper reaction region. Whereas in the lower RDWC, the MeOH recovery occurred above the reaction region and DEC could easily be removed as a bottom product in the reaction region because pure DEC is the only stable node in this system. The temperature profile of the middle of the RD column in the upper and the lower RDWC are also different. The upper RDWC has a higher temperature region from stages 4 to 46 than the lower RDWC as shown in Fig. 4(a) and Fig. 5(a) because the reaction region is positioned in the top of the RD column, and carbonate components of EMC and DEC with higher boiling points are produced in the reaction region.

These tendencies of reflux ratios and temperature distributions

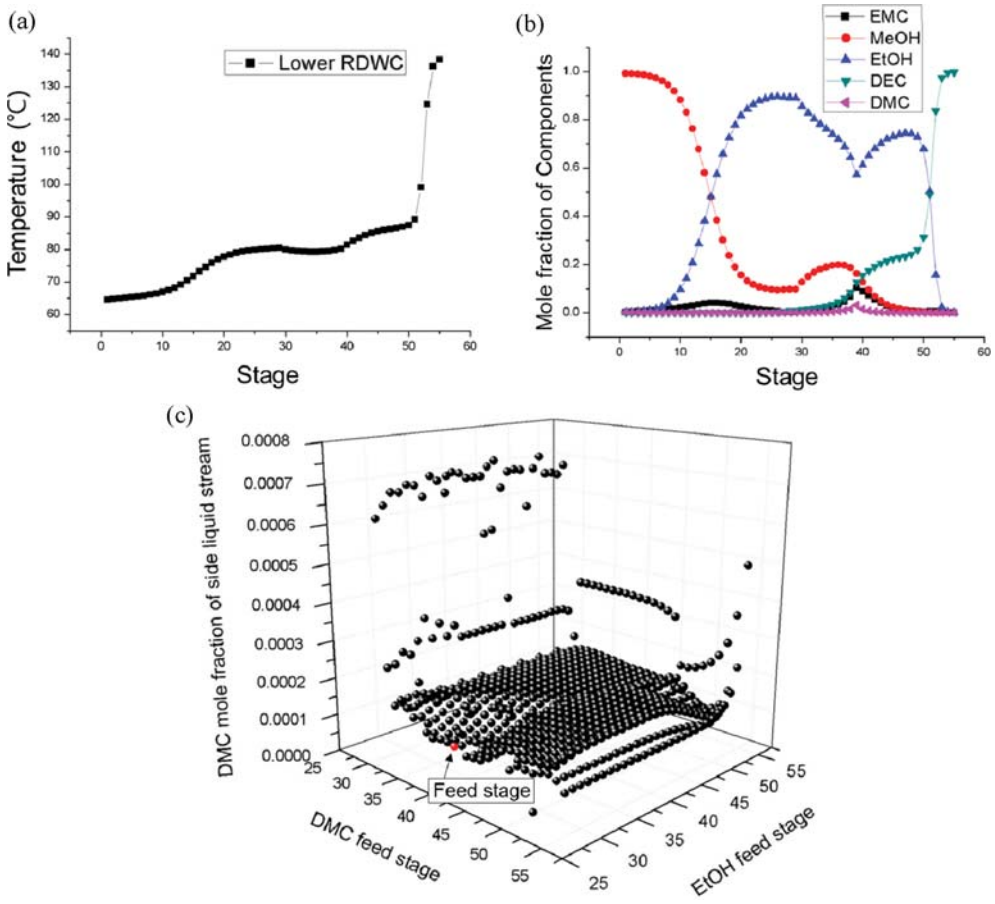

Fig. 5. (a) The temperature profile and (b) the composition profile in the RD column of the lower RDWC, and (c) sensitivity results of the DMC mole fraction of the side liquid stream according to the change of the DMC and the EtOH feed stages.

are reflected in the energy consumption of the RDWCs as the heat duty of the reboiler and condenser. The total energy consumption (Q_{total}) in the upper and lower RDWC was calculated by the following equations:

$$\text{In case of the upper RDWC, } Q_{Total} = -Q_{C1} + Q_{R1} - Q_{C2} \quad (5)$$

$$\text{In case of the lower RDWC, } Q_{Total} = -Q_{C1} + Q_{R1} + Q_{R2} \quad (6)$$

where Q_{C1} and Q_{R1} are the condenser duty and the reboiler duty in the reactive section and Q_{C2} and Q_{R2} are the condenser duty and the reboiler duty in the EtOH recovery section. The minus sign in front of both Q_{C1} and Q_{C2} is to correct the negative condenser duty value. According to the calculated results in Table 3, the required Q_{Total} of the upper RDWC is 9,617.70 kW, which is 35% higher than the lower RDWC because of a higher reflux ratio due to the high temperature profile.

The total annual cost (TAC) is also calculated with a payback period of three years in Eq. (7):

$$\text{TAC} = \frac{\text{Total capital cost}}{3} + \text{Total utility cost} \quad (7)$$

We calculated both the total capital cost and the total utility cost using the built-in equation in Aspen Plus™. The cost data of utilities and the detailed results of the total capital cost are shown in the Supporting Information (Tables S1 and S2). The TAC of the upper RDWC was 32.5% higher than that in the lower RDWC. Therefore, the production of DEC in the RDWC should be designed in the lower RDWC.

However, for the DEC production system, the separation of all products with a high purity in a single column shell is still limited in terms of the energy consumption. Even the lower RDWC has to secure a sufficient number of stages and a reflux ratio for pure MeOH recovery because the reacting mixture has an azeotropic unstable node between MeOH and DMC. The lower RDWC also still requires significant heat duties at two bottom reboilers and one top condenser. Therefore, a more energy-efficient design is needed for the DEC production.

2-2. Optimization of the Lower RDWC for the DEC Production System

Before the improvement of the lower RDWC, it was optimized to minimize the TAC and Q_{Total}. The equivalent scheme of the lower RDWC for the optimization consists of the RD column (C1) and the EtOH recovery column (C2), which is shown in Fig. 2(b).

In order to propose a procedure for the optimization, the lower RDWC was divided into three parts: the number of stages of the reactive section (N_{RX}), the non-reactive rectifying section for MeOH recovery (N_{REC}), and the non-reactive EtOH recovery section (NT_2). The optimization parameters of the RD column are N_{RX}, N_{REC} and

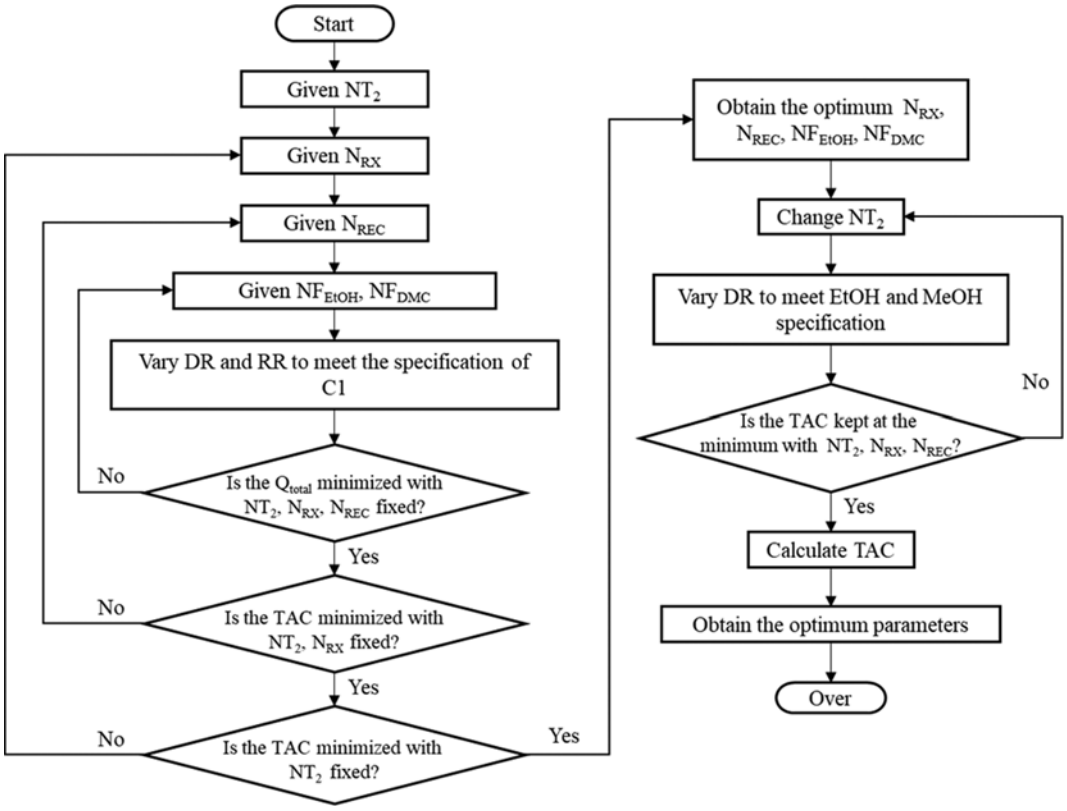

Fig. 6. Optimization procedure of the lower RDWC.

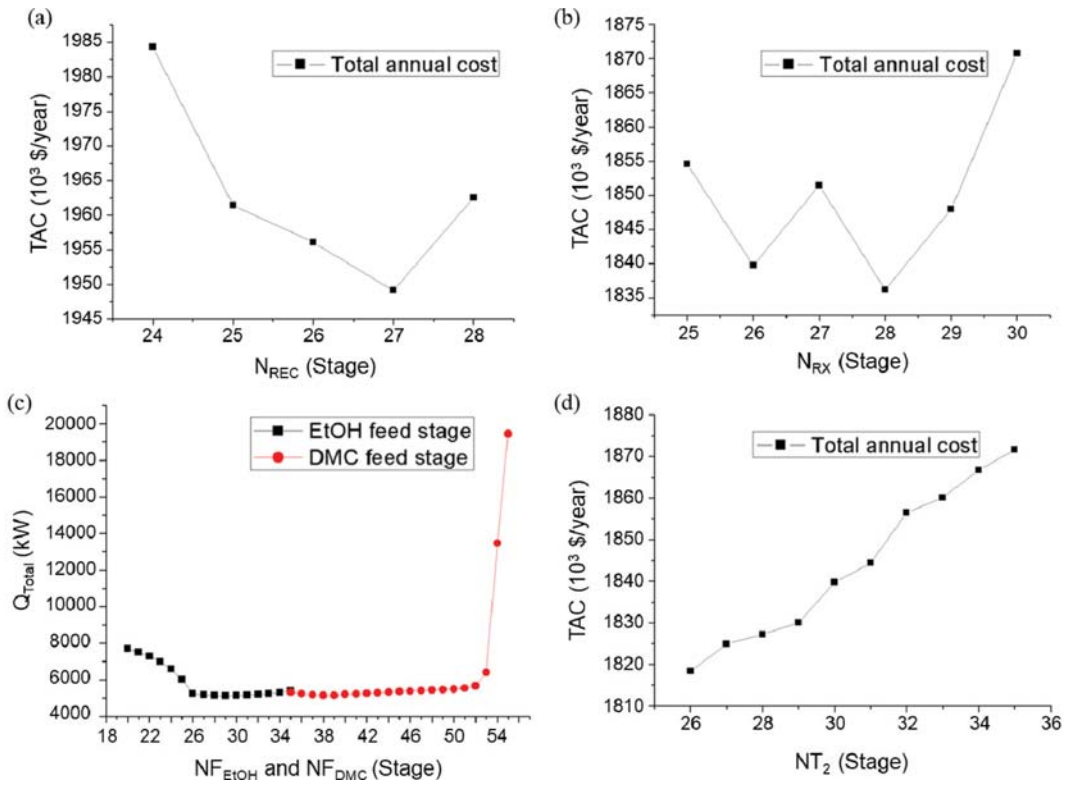

Fig. 7. The optimization results of the number of stages (a) in the reaction region (N_{RX}); (b) in the rectifying region (N_{REC}); (c) the feed stages of EtOH (NF_{EtOH}) and DMC (NF_{DMC}); and (d) the number of stages in the EtOH recovery column denoted by NT_2 in the lower RDWC.

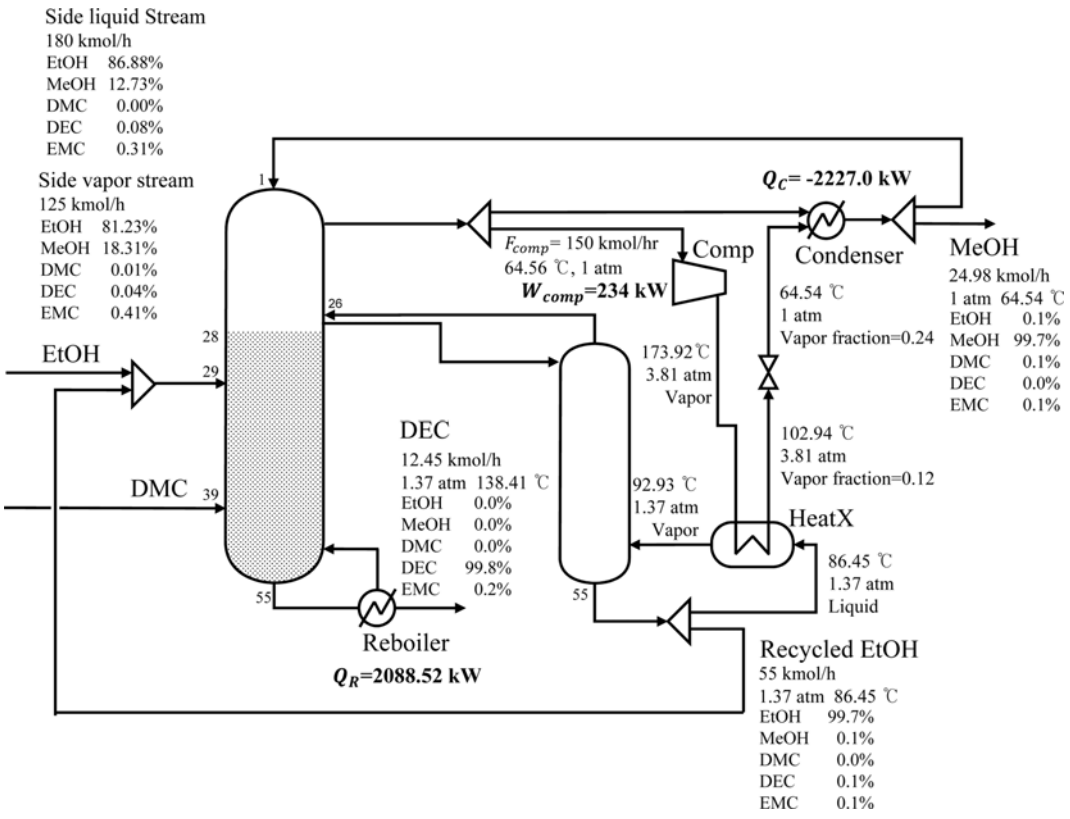

Fig. 8. The optimization results of the VRHP integrated RDWC.

the feed stages of EtOH and DMC, denoted as NF_{EtOH} and NF_{DMC}, respectively. Both N_{RX} and N_{REC} were optimized to minimize TAC while both NF_{EtOH} and NF_{DMC} were determined to minimize Q_{Total} because the feed stage of reactants affects the composition profile behavior and heat duties to separate pure MeOH. The optimization variable, NT_2 of the EtOH recovery column, was obtained by minimizing TAC. The optimization procedure for the lower RDWC is illustrated in Fig. 6.

Optimization results of N_{RX} and N_{REC} are presented in Figs. 7(a) and (b). The optimized values of N_{RX} and N_{REC} are 28 and 27, respectively. Accordingly, the total stage number of the RD column was determined as 55. The optimization results of NF_{EtOH} and NF_{DMC} for minimizing Q_{Total} are shown in Fig. 7(c) within the range of the feed stages for giving a DMC mole fraction of less than 10^{-4} in the side liquid stream. The optimal feed stage of EtOH is 29, while the optimal DMC-feed stage is 39 for a minimum heat consumption. As NT_2 increases, the TAC is also raised proportionally. The minimum value of NT_2 is 29 for the recovery of EtOH with the purity of 99.7%. The optimized amount of EtOH recycled into the RD column was used as 55 kmol/h [21].

3. Design and Optimization for the VRHP Integrated RDWC

3-1. Design of the VRHP Integrated RDWC

The VRHP was integrated into the lower RDWC to significantly reduce the energy consumption. Prior studies mainly applied the VRHP to non-reactive systems or single reaction RD systems [23-26], but this study introduced the VRHP to the DEC production system having the consecutive two reactions in the lower RDWC. The overhead vapor stream enters the VRHP and is compressed to heat the bottom EtOH stream as shown in Fig. 8.

The overhead vapor stream in the reactive section was divided by a splitter at a proper flow rate and was sufficiently compressed to be used as a heat source for reboiling the bottom liquid of the EtOH recovery column. As a result, the latent heat of the pressurized overhead vapor stream was provided for vaporizing the EtOH stream. The bottom liquid was totally vaporized and the partially liquefied overhead gas stream was completely liquefied by an auxiliary condenser after passing through the valve. Thus, the excessive reduction of energy consumption and utility usage occurred by reducing the heat duties of the reboiler in the non-reactive section and the condenser in the reactive section.

The total energy consumption of the VRHP integrated RDWC is defined as follows:

$$Q_{total}=Q_{R1}+W_{comp}-Q_C \tag{8}$$

Q_C is the condenser duty in the coupled VRHP system. The type of compressor in the VRHP was isentropic using an ASME method and the isentropic efficiency was set to 0.75. Detailed column specifications and operating conditions are shown in Table 4.

The TAC is calculated by Eq. (7) and the investment cost of the compressor is estimated as follows [26]:

$$\text{Investment cost of compressor} = \frac{M\&S}{280}\times 1264.75\times \text{horsepower}^{0.82} \tag{9}$$

The value of Marshall and Swift (M&S) index for the compressor is 1293 [26]. The calculated investment cost of the compressor

Table 4. Operating conditions for simulations of the bare lower RDWC and the VRHP integrated RDWC

Parameter	The bare lower RDWC	The VRHP integrated RDWC
Condenser pressure of C1 [atm]	1	1
1st stage pressure of C2 [atm]	1.173	1.166
Pressure drop [kPa]	0.7	0.7
Distillate rate [kmol/h]	24.97	24.98
Reflux ratio	12.5	12.64
Bottoms rate of C1 [kmol/h]	12.46	12.45
Liquid split ratio	0.6315	0.624

Table 5. Comparisons of the energy consumption and the TAC between the lower RDWC and the VRHP integrated RDWC

Parameter	Lower RDWC	the VRHP integrated RDWC
DEC purity [mol%]	99.7	99.8
MeOH purity [mol%]	99.7	99.7
EtOH purity [mol%]	99.7	99.7
Q_{C1} [kW]	−3301.47	-
Q_{R1} [kW]	2051.16	2088.53
Q_{R2} [kW]	1345.73	-
F_{comp} [kmol/h]	-	150
W_{comp} [kW]	-	234
Q_C [kW]	-	−2227.01
Q_{Total} [kW]	6698.36	4549.54
Total capital cost ($10^3$$)	2371.2	2735.12
Total utility cost ($10^3$$/yr)	1039.67	815.442
TAC ($10^3$$/yr)	1830.07	1727.15

and the other detailed result of the TAC for the VRHP integrated RDWC are given in the Supporting Information (Table S2). As shown in Table 5, the integration of the VRHP lowered the Q_{Total} by 32.1% compared to the bare lower RDWC. The VRHP exchanges the heat of 1,346.71 kW between the overhead MeOH vapor and the bottom EtOH liquid. For the cost evaluation, the total capital cost increased due to the installation of the VRHP, but the total utility cost decreased by 21.6%. Overall, the TAC decreased with the integration of the VRHP.

3-2. Optimization of the VRHP Integrated RDWC

We based the optimization of the VRHP integrated RDWC on the procedure of the bare lower RDWC. However, the optimization procedure of the EtOH recovery column considered the integration of the VRHP because the VRHP completely replaces the reboiler of the EtOH recovery column. The optimization procedure of the VRHP integrated RDWC is illustrated in Fig. 9.

The optimization procedure minimizes the power consumption of the compressor (W_{comp}) with respect to the gas flow rate (F_{comp}) of the MeOH vapor stream to the compressor. The results of the optimized VRHP system are shown in Fig. 8. W_{comp} is defined as the minimum work required for the compressor to fully vaporize the bottom liquid with the overhead stream of a given F_{comp}. Consequently, the optimal F_{comp} is 150 kmol/h for the minimum W_{comp}.

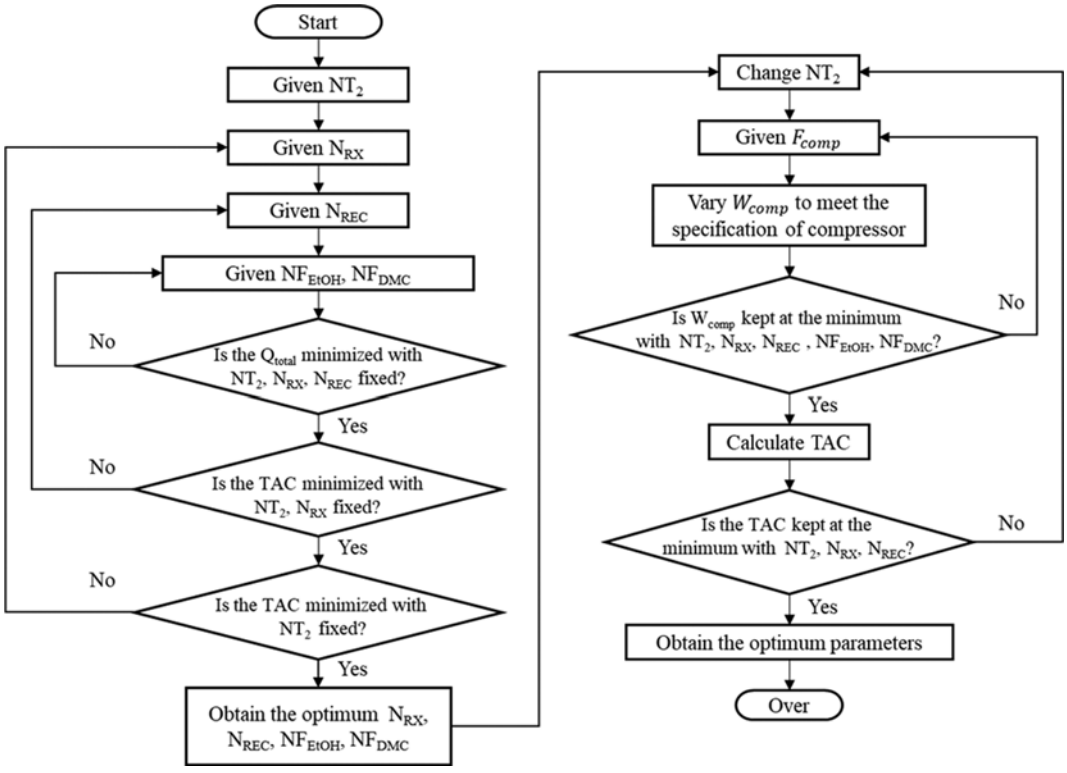

Fig. 9. Optimization procedure of the VRHP integrated RDWC.

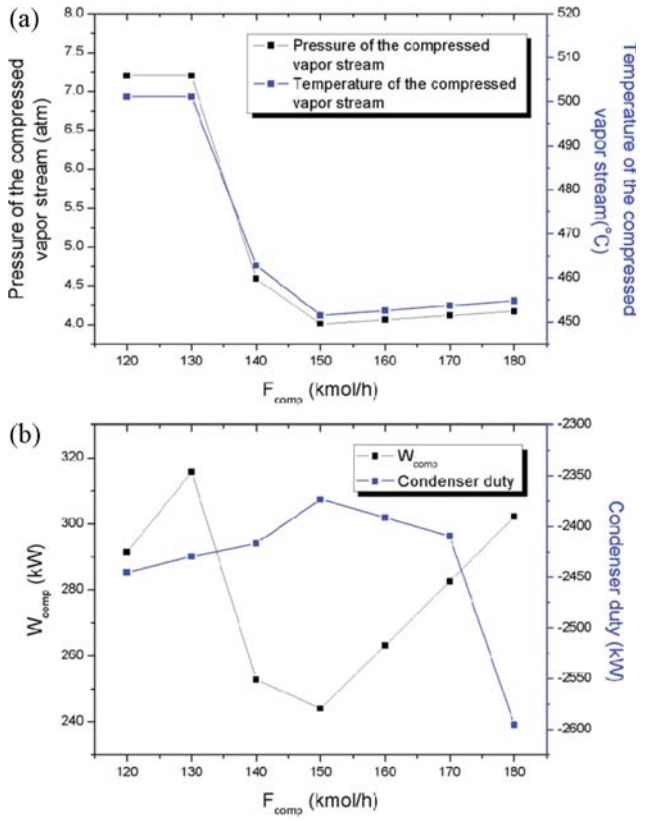

Fig. 10. The optimization results of (a) the pressure and temperature of the overhead vapor stream; and (b) the power consumption of the compressor and the condenser duties according to the F_{comp} in the VRHP, respectively.

The pressure of the overhead MeOH stream was increased to fully vaporize the bottom EtOH stream due to the lower boiling MeOH point at the same pressure. To verify the influence of the vapor flow rate into the compressor (F_{comp}), we investigated the change in the temperature and pressure of the compressed overhead vapor as illustrated in Fig. 10. The temperature and pressure of the stream rapidly decreased until F_{comp} was 150 kmol/h, but then gradually increased above 150 kmol/h as shown in Fig. 10(a). This temperature behavior signifies that the temperature difference between the overhead and the bottom stream does not change below 100 °C even if F_{comp} increases. Fig. 10(b) shows that W_{comp} has a minimum value at F_{comp} of 150 kmol/h. Likewise, the condenser also requires the lowest duty at 150 kmol/h for the liquefaction of the overhead MeOH stream.

As a result, DEC and MeOH were respectively obtained with a purity of 99.8% and 99.7% while EtOH was recycled into the reaction region with a purity of 99.7%. The liquid composition trajectory in the RD column is shown in Fig. 11. The reactant DMC existed with a molar fraction of less than 0.001 in most stages of the rectifying region and less than 0.005 in the reaction region except near the DMC feed stage because it was reacted with the excess EtOH. In the top rectifying section, there is a trace amount of EMC because the boiling point of EtOH-EMC azeotrope is 77.9 °C and higher than the boiling point of the azeotropic unstable node at 63.7 °C. Consequently, EMC does not affect the purity of the MeOH

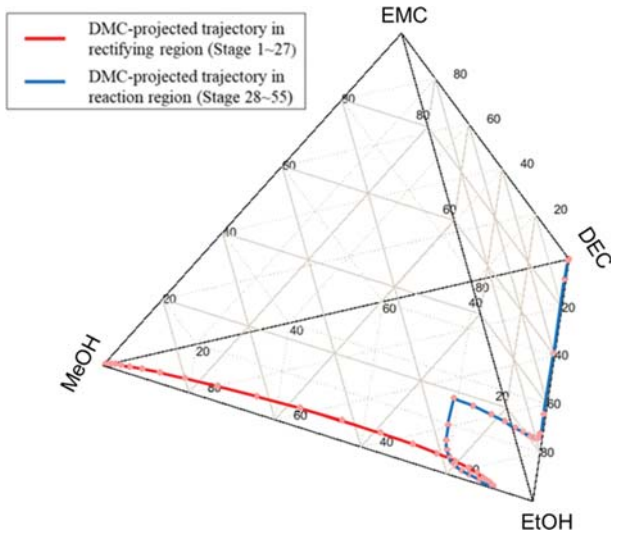

Fig. 11. The liquid composition trajectory projected onto a DMC in the RD column of the VRHP integrated RDWC. The blue line represents the reaction region from 28th stage to the 55th stage, while the red line represents the non-reactive rectifying region from 1st stage to the 27th stage.

stream, and the separation of MeOH and EtOH occurs in the non-reactive section against the dividing wall. The excessive amount of EtOH was partially consumed in the reaction region while the mole fraction of EMC and MeOH increased simultaneously by the reactions. As the stage moves down to the bottom in the reactive section from stage 28 to 55, the trajectory approached the binary edge between EtOH and DEC. Therefore, the pure DEC can be produced at the bottom of the RD column.

CONCLUSION

The lower RDWC for the DEC production was verified to be a more energy-efficient structure than the upper RDWC. The system with a minimum azeotropic unstable node between the light desired product and the heavy reactant makes the feed stage position of the heavy reactant as a crucial optimization variable. Thus, we conducted a sensitivity analysis on the DMC mole fraction above the reaction region according to the location of reactant feed stages to produce products with high purity. However, there was a limit to the reduction of energy consumption in the RDWC because the reaction of DMC with EtOH and the recovery of EtOH and MeOH occurred in only one column shell. Therefore, the integration of the VRHP into the lower RDWC dramatically reduced the energy consumption despite the presence of the consecutive multi-component reactions. Moreover, the VRHP was optimized with respect to the gas influx into the compressor. As a result, DEC and MeOH were obtained with high purities of 99.8% and 99.7%, respectively. The energy consumption decreased by 32.1% and the total utility cost was also cut by 21.6% compared to the bare lower RDWC case.

ACKNOWLEDGEMENTS

The authors are grateful for the financial support from the Han-

wha Chemical R&D Institute through the KAIST-Hanwha Future Technology R&D Center. This research was also supported by Engineering Development Research Center (EDRC) funded by the Ministry of Trade, Industry & Energy (MOTIE) (No. N02180129).

NOMENCLATURE

C1 : reactive distillation column [-]
C2 : EtOH recovery column [-]
Comp : vapor compressor [-]
DEC : diethyl carbonate [-]
DMC : dimethyl carbonate [-]
DR : distillate rate [kmol/h]
EMC : ethyl methyl carbonate [-]
EtOH : ethanol [-]
F_{comp} : flow rate to vapor compressor [kmol/h]
HeatX : heat exchanger [-]
MeOH : methanol [-]
N_{RX} : number of reactive stage for C1 [-]
N_{REC} : number of rectifying stage for C1 [-]
NF_{DMC} : DMC feed location [-]
NF_{EtOH} : EtOH feed location [-]
NT_n : theoretical number of plates for column n [-]
Q_C : heat duty of a condenser in VRHP [kW]
Q_{Cn} : heat duty of a condenser in column n [kW]
Q_{Rn} : heat duty of a reboiler in column n [kW]
Q_{Total} : the amount of total heat consumption [kW]
RD : reactive distillation [-]
RDWC : reactive dividing wall column [-]
RR : reflux ratio [-]
S : saddle [-]
SN : stable node [-]
TAC : total annual cost [$10^3$$/yr]
UN : unstable node [-]
VRHP : vapor recompression heat pump
W_{comp} : power consumption applied to the compressor [kW]

SUPPORTING INFORMATION

Additional information as noted in the text. This information is available via the Internet at http://www.springer.com/chemistry/journal/11814.

REFERENCES

1. M. A. Gadalla, Z. Olujic, P. J. Jansens, M. Jobson and R. Smith, *Environ. Sci. Technol.*, **39**, 6860 (2005).
2. J. Park, R. H. Kang and J. W. Lee, *Korean J. Chem. Eng.*, **34**, 1763 (2017).
3. R. H. Kang, J. Park, D. Kang and J. W. Lee, *Korean J. Chem. Eng.*, **35**, 734 (2018).
4. J. Zhang and J. W. Lee, *Carbon*, **53**, 216 (2013).
5. J. Zhang, Z. Yu, D. Atkins and J. W. Lee, *J. Phys. Chem. C*, **115**, 8386 (2011).
6. Y. K. Kim, G. M. Kim and J. W. Lee, *J. Mater. Chem. A*, **3**, 10919 (2015).
7. X. Gao, X. Yin, S. Yang and D. Yang, *Korean J. Chem. Eng.*, **36**, 77 (2019).
8. Y. H. Kim, *Korean J. Chem. Eng.*, **33**, 2513 (2016).
9. N. V. D. Long and M. Y. Lee, *Korean J. Chem. Eng.*, **30**, 286 (2013).
10. J. J. Siirola, AIChE Symposium Series, New York, NY: American Institute of Chemical Engineers, **91**, 222 (1995).
11. M. F. Malone and M. F. Doherty, *Ind. Eng. Chem. Res.*, **39**, 3953 (2000).
12. Z. Guo, M. Ghufran and J. W. Lee, *AIChE J.*, **49**, 3161 (2003).
13. Z. Guo and J. W. Lee, *AIChE J.*, **50**, 1484 (2004).
14. J. Chin, J. W. Lee and J. Choe, *AIChE J.*, **52**, 1790 (2006).
15. D. Kang and J. W. Lee, *Korean Chem. Eng. Res.*, **52**, 713 (2014).
16. D. Kang and J. W. Lee, *Comput. Aided Chem. Eng.*, **34**, 351 (2014).
17. S. H. Lee, W. Y. Choi, K. J. Kim, D. J. Chang and J. W. Lee, *Chem. Eng. Process.*, **123**, 249 (2018).
18. D. An, W. Cai, M. Xia, X. Zhang and F. Wang, *Chem. Eng. Process.*, **92**, 45 (2015).
19. D. Kang and J. W. Lee, *Ind. Eng. Chem. Res.*, **54**, 3175 (2015).
20. I. Mueller and E. Y. Kenig, *Ind. Eng. Chem. Res.*, **46**, 3709 (2007).
21. L. Zheng, W. Cai, X. Zhang and Y. Wang, *Chem. Eng. Process.*, **111**, 127 (2017).
22. J. Chin and J. W. Lee, *Ind. Eng. Chem. Res.*, **47**, 3930 (2008).
23. X. Gao, Z. Ma, L. Yang and J. Ma, *Ind. Eng. Chem. Res.*, **52**, 11695 (2013).
24. Z. Zhu, X. Liu, Y. Cao, S. Liang and Y. Wang, *Korean J. Chem. Eng.*, **34**, 866 (2017).
25. S. Feng, X. Lyu, Q. Ye, H. Xia, R. Li and X. Suo, *Ind. Eng. Chem. Res.*, **55**, 11305 (2016).
26. S. Feng, Q. Ye, H. Xia, R. Li and X. Suo, *Chem. Eng. Res. Des.*, **125**, 204 (2017).
27. J. A. Ferre, F. Castells and J. Flores, *Ind. Eng. Chem. Process Des. Dev.*, **24**, 128 (1985).
28. A. Rodrıguez, J. Canosa, A. Domínguez and J. Tojo, *Fluid Phase Equilib.*, **201**, 187 (2002).
29. A. Rodríguez, J. Canosa, A. Domínguez and J. Tojo, *J. Chem. Eng. Data*, **48**, 86 (2003).
30. X. Zhang, J. Zuo and C. Jian, *J. Chem. Eng. Data*, **55**, 4896 (2010).
31. H.-P. Luo, W.-D. Xiao and K.-H. Zhu, *Fluid Phase Equilib.*, **175**, 91 (2000).
32. NIST Chemistry WebBook. http://webbook.nist.gov/chemistry/.
33. H.-P. Luo and W.-D. Xiao, *Chem. Eng. Sci.*, **56**, 403 (2001).
34. T. Keller, J. Holtbruegge, A. Niesbach and A. Górak, *Ind. Eng. Chem. Res.*, **50**, 11073 (2011).
35. J. W. Lee, Y. Ko, Y. Jung, K. Lee and E. Yoon, *Comput. Chem. Eng.*, **21**, S1105 (1997).
36. M. F. Doherty, *Chem. Eng. Sci.*, **40**, 1885 (1985).
37. H.-Y. Wei, A. Rokhmah, R. Handogo and I. L. Chien, *J. Process Control.*, **21**, 1193 (2011).